

ARTICLES

The Relationship between El Niño and the Duration and Frequency of the Santa Ana Winds of Southern California

Jason Finley and Marilyn Raphael

University of California, Los Angeles

This study examines the variability of the duration and frequency of Santa Ana winds due to El Niño over a thirty-three-year period. *Daily Weather Maps* and NCEP/NCAR Reanalysis were used to study large-scale upper-level and surface circulation patterns during wind events. A Student's *t*-test was used to determine statistically significant changes in the winds during March of El Niño winters. A significant decrease in the duration and frequency of wind events was found in March during El Niño. This can be attributed to the decrease in strength and frequency of the Great Basin high pressure and the increase in wintertime cyclones in southern California. **Key Words:** California, El Niño, Santa Ana winds.

Santa Ana winds are dry, downsloping, north-easterly winds that warm adiabatically as they descend in the lee of a mountain between September and early May in southern California. These winds are similar to those observed in the lee of Colorado's Front Range and in the Inn Valley of Austria (Fosberg, O'Dell, and Schroeder 1966).

The Santa Ana event frequency is relatively low in September but peaks in December with a monthly average of 3.5 events (Raphael 2003). The monthly frequency then consistently decreases over the winter and early spring months. No event is found between June and August due to the dominant Pacific high pressure patterns situated west of California and the associated westerly flows that move into the region and inhibit northeasterly winds in southern California.

The timing of these winds following the typical dry summers of California's Mediterranean climate can also create a serious fire hazard. National forest fire data reveal that most large fire outbreaks are sparked by strong north-easterly Santa Ana winds between September and April (Minnich 1983). Fire behavior is affected by many meteorological elements, including wind speed and relative humidity (Fosberg, O'Dell, and Schroeder 1966). Relative humidity during Santa Ana wind events has been observed to decrease to less than 5 percent in a period of four hours (Sommers 1978). This

combination of the Santa Ana winds' low relative humidity and high wind speeds produces one of the most extreme fire dangers in the world (Fosberg, O'Dell, and Schroeder 1966).

Several studies have analyzed the synoptic-scale circulation conducive to the development of Santa Ana winds. Older studies, such as that of Fosberg, O'Dell, and Schroeder (1966), found the synoptic aspects of Santa Ana winds to include a surface low pressure trough offshore near central or southern California and an anticyclone in the Great Basin (see Figure 1A). Sommers (1978) used the Limited Fine Mesh model to better understand the synoptic-scale conditions during Santa Ana winds for forecasting techniques. The combination of the north-south to west-northwest-east-southeast orientation of the southern California mountains and the crucial lee of the mountains on the west necessitates a well-developed, meridional component of the midtropospheric systems to provide moderate winds perpendicular to the mountains (Sommers 1978). Strong windward static stability and an upstream inversion also appear to be associated with Santa Ana winds, which is consistent with Klemp and Lilly's (1975) findings. The duration of the Santa Ana winds depends strongly on the duration of the 500-mb ridge/trough (R/T) pattern over the western United States. The R/T pattern represents a strong ridge over the west coast and a

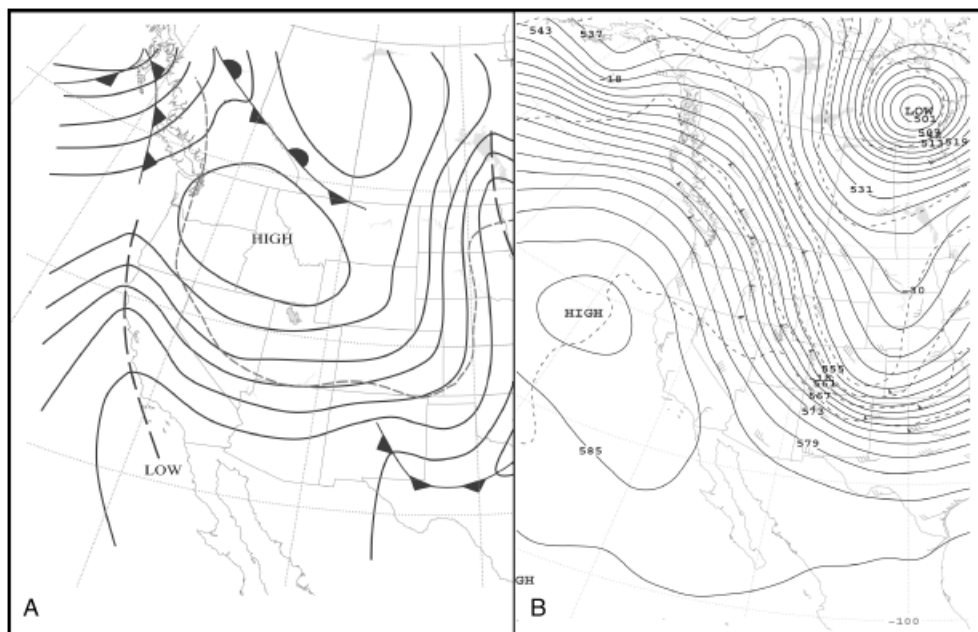


Figure 1 Large-scale circulation patterns of the Santa Ana wind event on 15 November 2005 at 4 a.m. PST. The diagram at the left (A) is the synoptic-scale sea-level pressure pattern of the coupled high and low pressure patterns. The diagram at the right (B) is the 500-mb geopotential height pattern that shows the strong ridge over the west coast of North America and the trough that digs southward toward Arizona and New Mexico. This pattern is an example of the ridge/trough (R/T) pattern typically found during Santa Ana wind events.

trough that digs southward toward Arizona and New Mexico (see Figure 1B). These patterns are carefully examined since the wind events end when the 500-mb flow becomes more zonal or when a new trough position becomes established west of California (Sommers 1978).

Although extensive studies (Fosberg, O'Dell, and Schroeder 1966; Scheetz, Henz, and Maddox 1976; Sommers 1978) have provided well-documented descriptions of the nature and importance of the synoptic-scale meteorological conditions that produce the Santa Ana winds, there has been little research on the variability of the frequency of events on interannual and longer time scales. Raphael (2003) calculated the average duration and frequency of Santa Ana events per year from *Daily Weather Maps* (1968–2000; data set details are given in the following section). She noted that there exists a substantial interannual variation in the frequency and duration of events and that a relationship between El Niño Southern Oscillation (ENSO) and

Santa Ana event frequency may exist. Her initial statistical analysis of the Santa Ana events during the warm phase of ENSO (El Niño) revealed a temporal decrease in the number of events but an increasing number of days per event. Comparison of the Southern Oscillation index (SOI) with the monthly and seasonal frequency of the Santa Ana winds revealed a correlation mostly in February and March (Raphael 2003).

El Niño is characterized by an increase in the sea surface temperatures (SST) in the tropical waters of the eastern and central Pacific Ocean every two to seven years. It is linked to the negative phase of the Southern Oscillation, when lower surface atmospheric pressure is observed off the coast of South America due to warmer waters and higher atmospheric pressure is observed near Australia and Indonesia (Goude 2001). The global impacts of El Niño can include droughts in southern India and Indonesia, flooding in Peru, and heavy precipitation

in the southeastern United States and California (Ropelewski and Halpert 1987). The cold phase of ENSO, known as La Niña, is characterized by cooler than normal SST in the eastern Pacific, and its global atmospheric/oceanic effects are generally opposite to those of El Niño. However, since the east-west scale of rainfall anomalies in the tropical Pacific is reduced compared to El Niño, the changes to the global climate (and to the climate in southern California) are not as dramatic compared to those observed during El Niño (Fedorov and Philander 2000).

El Niño influences three primary components of the midtropospheric circulation during winter in the northern hemisphere. One is a fairly stationary Pacific–North American wave (Livezey et al. 1997) extending from tropical to subtropical latitudes across the eastern Pacific and the southern United States. Another is a more intensified and expansive Aleutian Low connected to the development of the stationary Pacific–North American pattern (Schonher and Nicholson 1989). The third component is the strengthening of the subtropical flow persistently located across the southern United States. The amplification of this flow is related to an increased northward flux of angular momentum, resulting from the enhanced Hadley circulation in the eastern Pacific Ocean during El Niño (Schonher and Nicholson 1989). Since the Aleutian Low extends toward the California coast and the midlatitude storm track extends farther south toward the southern United States, intense winter storms in southern California are more frequent during El Niño winters (Raphael and Mills 1996). The higher frequency of strong surface-to-midlevel onshore flow associated with these winter storms can modify the mean synoptic-scale patterns over the southwestern United States. The increase in storms may inhibit the formation and possibly reduce the longevity of strong high-pressure systems in the Great Basin and disrupt the coupling of the high and low pressure patterns across the region, thereby influencing the strength and/or frequency of the Santa Ana winds. Based on this and previous research, we believe that a relationship between El Niño and the frequency of winter season events exists.

The goal of this study is to examine further the interannual variability of the Santa Ana winds by focusing on the influence El Niño

has on the duration and frequency of the wind events. The study examines the spatial and temporal variations of the large-scale surface and 500-mb flow patterns among El Niño and non-El Niño years in the western United States. La Niña years are included in the non-El Niño category. We focus on El Niño years because the atmospheric dynamics associated with El Niño appear to have clearer consequences for the duration and frequency of Santa Ana events. However, the influence of La Niña on the Santa Ana winds could be the subject of further study.

Data and Methods

The first data set used in this study is Raphael's (2003) tabulated collection of Santa Ana days. This data set was used for determining averages of duration and frequency of Santa Ana events (see Table 1), and was the basis for determining which days to analyze the surface and 500-mb circulation patterns. Raphael's collection is based on analyzing synoptic weather maps that were extracted from the *Daily Weather Maps* (1968–2000). These daily maps represent the weather patterns at 4 a.m. PST (Pacific Standard Time) when the Santa Ana wind is not hindered by the opposing sea breeze circulation (cf. Figure 1A). The land breeze is typically much weaker than the sea breeze in this region; however, for this particular study, the strength of the

Table 1 Frequency (events/month), duration (days/events), and mean number of days for each month for the Santa Ana winds and the associated ridge/trough patterns

Month	El Niño	Non-El Niño	El Niño	Non-El Niño
	Santa Ana frequency		Ridge/trough frequency	
November	3.14	3.46	2.00	1.58
December	3.85	3.42	2.00	1.67
January	3.43	3.17	1.85	1.58
February	2.72	2.79	1.42	1.17
March	1.14	2.00	0.57	0.88
	Santa Ana duration		Ridge/trough duration	
November	2.09	1.88	1.18	1.28
December	2.14	2.10	1.73	1.39
January	2.12	2.37	1.45	1.57
February	1.43	1.52	1.24	1.35
March	1.35	1.64	1.31	1.56
	Santa Ana days		Ridge/trough days	
November	6.56	6.50	2.36	2.02
December	8.24	7.18	3.46	2.32
January	7.27	7.51	2.68	2.48
February	3.89	4.24	1.76	1.58
March	1.54	3.28	0.75	1.37

land/sea breeze should have no influence on the duration and frequency of the Santa Ana event. Raphael's criteria for selecting Santa Ana days included the simultaneous existence of a Great Basin high and a California coastal low as well as a prevailing wind in the northeastern quadrant at Los Angeles. The pressure distribution was examined carefully to determine which days met the above criteria. These patterns resulted in positive central pressure differences ranging from 4 to 28 mb between the Great Basin high pressure and the offshore low pressure systems. Days in which these systems did not exist in tandem were not considered Santa Ana days. This data set was created qualitatively due to the often vague boundaries of the high and low pressure systems that can result when using objective methods (Raphael 2003).

The NCEP/NCAR Reanalysis data set (Kalnay et al. 1996) was then used to extract large-scale surface and 500-mb spatially-referenced data representing the circulation patterns during each Santa Ana event recorded from November to March in the above data set. These data sets do not include data during non-Santa Ana days. The Reanalysis products, created to avoid perceived climate changes that result from many changes in the Global Assimilation System over the past two decades, use a frozen, state-of-the-art analysis/forecast system. This allows for easy and flexible mapping of one variable at a time, as opposed to traditional daily weather maps that combine several variables on one map, hindering easy differentiation. The system also performs data assimilation of daily averages and four daily observations (4 p.m., 10 p.m., 4 a.m., 10 a.m. PST) of a wide array of pressure level and surface data variables. The output of the Reanalysis data is on 2.5×2.5 latitude-longitude grid covering the entire globe (Kalnay et al. 1996). For this study, the spatial and temporal domain was 110° – 130° W and 20° – 50° N in twelve-hour intervals.

The 500-mb geopotential height data of the R/T pattern within the spatial domain (described above and noted in Sommers's 1978 research) were obtained from the Reanalysis during each wind event. Averages of duration and frequency of these R/T patterns are given in Table 1. Sea-level pressure data showing the coupled high and low pressure patterns during the wind events were also obtained, and the

associated vertical velocity data (omega) were extracted to diagnose rising and sinking (subsiding) air between the surface and the 500-mb pressure level. Subsidence is important in analyzing the Great Basin high pressure as it typically occurs downstream of the 500-mb ridge, approximately above the surface high pressure. Rising air typically occurs upstream of the ridge above the coastal low pressure. Changes in omega are linked to changes in surface pressure. Positive (negative) values of omega represent subsidence (rising motion) at the 500-mb level, associated with an increase (decrease) in sea level pressure.

The geopotential height fields are strongly constrained by the assimilation of the observed data and are in the most reliable class of variables in the Reanalysis. Other variables, such as omega, are more dependent on model analysis and less on observational data (Kalnay et al. 1996). Caution may be needed in analyzing omega since model data are constructed using parameterizations and other assumptions that are not as reliable as direct observational data. In addition, the sea level pressure data in the Reanalysis does not consistently show boundaries of high and low pressure centers due to the relatively coarse resolution.

The mean of each Reanalysis variable at each grid point within the defined spatial extent was plotted for each month during El Niño and non-El Niño winters. The El Niño winters are defined as November–March of the following years: 1969–1970, 1972–1973, 1976–1977, 1982–1983, 1986–1987, 1991–1992, and 1997–1998 (Legler 1998). Legler chose these years using an index-based on the SST of the Niño 3 region. The index is a five-month running mean of SST anomalies averaged spatially over the tropical Pacific: 4° S– 4° N, 150° W– 90° W. The period of October of one year to September of the following year was categorized as an El Niño year if the index value for six consecutive months (including Oct.–Dec.) exceeded 0.5° C.

A Student's *t*-test with a 95 percent confidence interval was used to determine the statistical significance of the meteorological changes in the wind events throughout the Santa Ana season during El Niño. The *t*-test assumed that the data were spatially autocorrelated and that the two samples (El Niño and non-El Niño) have the same population

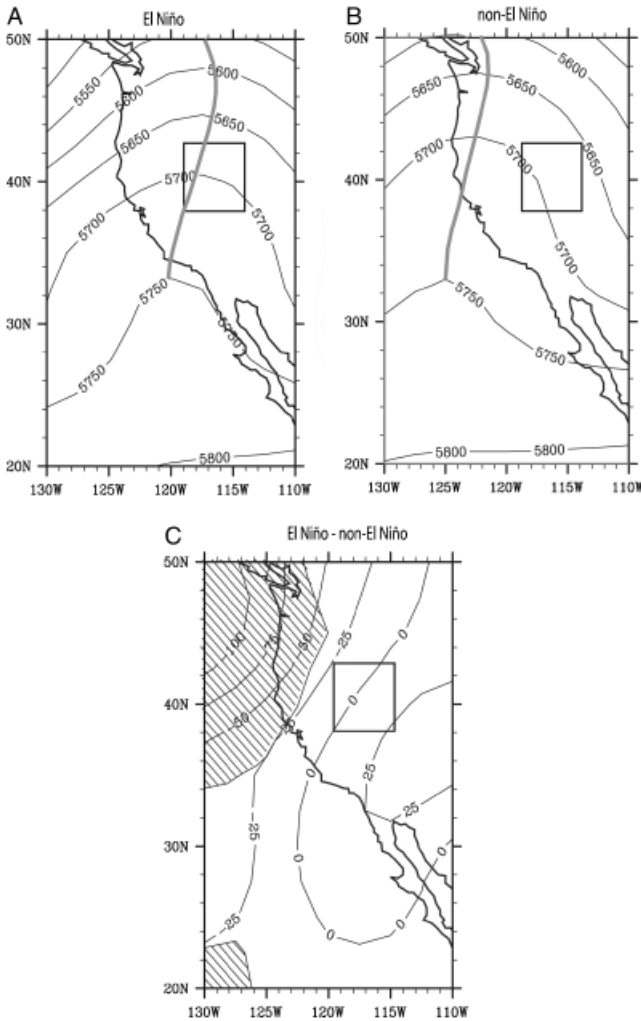


Figure 2 Mean geopotential height (gpm) during the Santa Ana wind events in March for (A) El Niño winters and (B) non-El Niño winters. Map C plots the difference between El Niño and non-El Niño winters, and the shaded areas in C denote the statistically significant differences ($\alpha < 0.05$). The rectangle is the general proximity of the Great Basin, and the thick, gray lines are the 500-mb ridge axes.

variance. The areas of statistically significant differences were superimposed onto the difference plots (e.g., Figures 2–4).

Results

Monthly Difference of Means

Table 1 consists of a set of statistics for the average frequency, the average duration, and the total number of days (product of frequency and duration) of the Santa Ana wind events and R/T patterns calculated separately for El Niño and non-El Niño winters for each month. It reveals

a steady decline in the frequency and mean duration of the Santa Ana events and of the R/T patterns from December to March, with a sharp drop in frequency of both variables in March. The differences between the means for El Niño and non-El Niño winters for November through February in Table 1 are small and inconsistent for both the wind events and the R/T patterns. These results may be a superposition of noise not physically linked to El Niño. However, there is a connection between the Santa Ana events and El Niño during March, as both the duration and frequency values of the Santa Ana winds during El Niño are smaller than

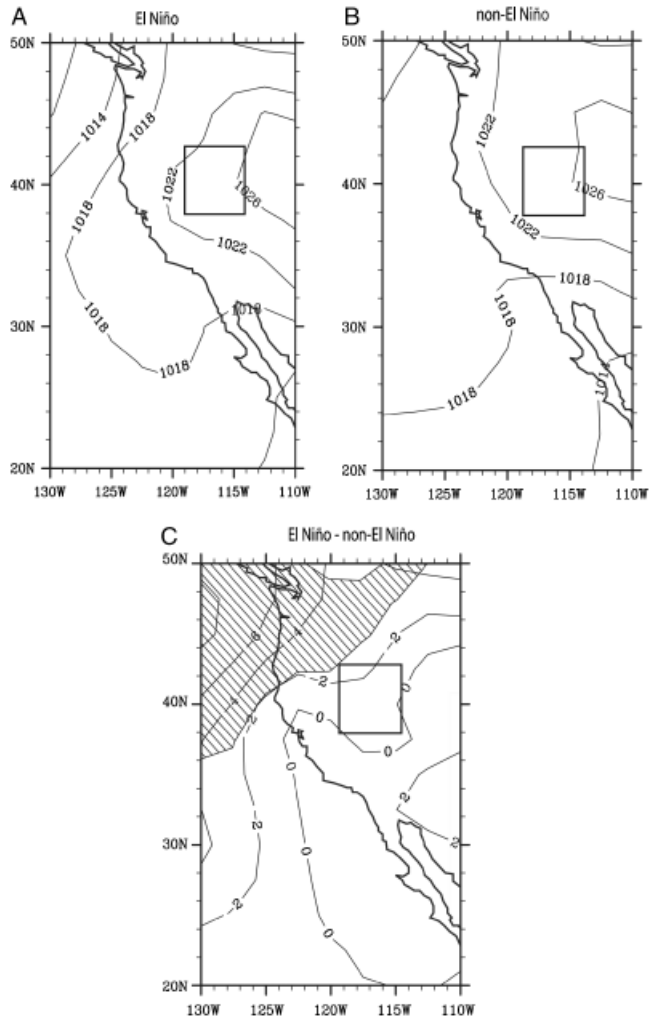


Figure 3 Mean sea level pressure (mb) during the Santa Ana wind events in March for (A) El Niño winters and (B) non-El Niño winters. Map C plots the difference between El Niño and non-El Niño winters, and the shaded areas in C denote the statistically significant differences ($\alpha < 0.05$). The rectangle is the general proximity of the Great Basin, and the thick, gray lines are the 500-mb ridge axes).

those during non-El Niño winters. For example, the mean number of Santa Ana days during non-El Niño winters for March is 3.28. The number of days per month for March during El Niño was reduced by 53 percent to only 1.54 days. These results are consistent with Raphael's (2003) preliminary analysis that suggested (but did not examine in detail) a decrease in frequency of events during late winter and a further decrease during El Niño.

Spatial Statistical Analysis

Due to the lack of significant differences between means for El Niño and non-El Niño winters for

November through February (in Table 1), the focus of the spatial analysis is on March. During El Niño winters, a more eastward displacement of the R/T axis is shown in Figure 2A when compared to the non-El Niño March pattern in Figure 2B. A statistically significant decrease in geopotential height is found over the northwestern United States (Figure 2C), indicating a further eastward advancement of the ridge. A new trough appears to enter the northwestern-United States and the region east of the ridge quickly after the onset of the Santa Ana winds. During March of non-El Niño winters, the ridge appears to dominate much of the western United

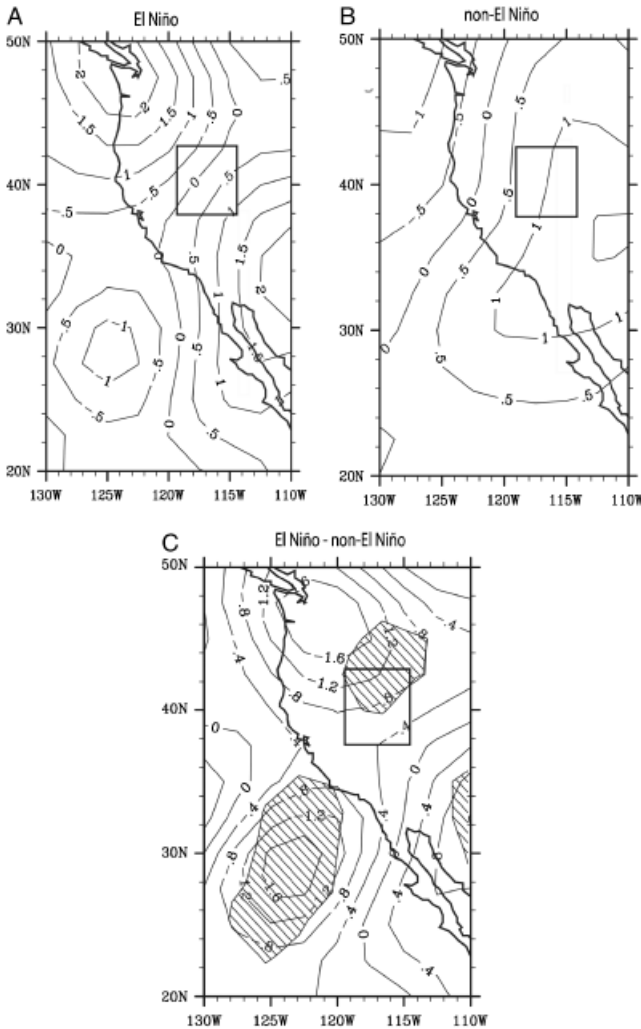


Figure 4 Vertical velocity data (*omega*; mb/s) during the Santa Ana wind events in March for (A) El Niño winters and (B) non-El Niño winters. Map C plots the difference between El Niño and non-El Niño winters, and the shaded areas in C denote the statistically significant differences ($\alpha < 0.05$). The rectangle is the general proximity of the Great Basin, and the thick, gray lines are the 500-mb ridge axes.

States throughout the wind events. This difference may represent a reduction in the duration of the ridge over the western United States during El Niño as a new trough begins to dominate. This would shorten the duration of the associated Great Basin high pressure and the accompanying Santa Ana wind events.

Figure 3B (non-El Niño winters) exhibits a decrease in sea level pressure in the northeastern Pacific and a small decrease in sea level pressure well west of California compared to Figure 3A (El Niño winters). The decrease in the northeastern Pacific is statistically significant (Figure 3C) and is most likely a result of the deepening

and expansion of the Aleutian Low toward the west coast of the United States (Schonher and Nicholson 1989). However, statistically significant changes in surface pressure in the Great Basin and in the pressure gradient over the southwestern United States during El Niño winters are not confirmed. This could be a result of the relatively coarse resolution of the surface pressure centers in the Reanalysis.

The El Niño patterns in March (Figure 4A) show weaker downward motion over part of the Great Basin compared to the patterns for non-El Niño winters (Figure 4B), which is statistically significant within the Great Basin region

(Figure 4C). This weaker downward motion can in turn weaken the northeast-to-southwest surface pressure gradient in the southwestern United States and shorten the Santa Ana events. In addition, stronger upward motion southwest of the southern California coast is evident during El Niño in Figure 4A. This is statistically significant over a large area of the offshore region during the events. The stronger uplift may be due to the increase of winter cyclones in southern California during El Niño winters, which, in turn, would shorten existing Santa Ana events and hinder the formation of new events.

Summary and Conclusions

Two main methods of analysis were used in examining the relationship between El Niño and the duration and frequency of the Santa Ana winds. The difference of means analysis between El Niño and non-El Niño winters in Table 1 and the spatial analyses in Figures 2–4 suggest a statistically significant decrease in the duration and frequency of the wind events in March during El Niño.

This damping of the March wind events during El Niño winters can be attributed to a faster progression of the R/T pattern over the western United States due to the strengthening of upper-level westerly flow and the deepening and expansion of the Aleutian Low. The R/T patterns may not form as frequently during El Niño, and those that do form may evolve and progress more quickly than during non-El Niño winters (Schonher and Nicholson 1989). The faster speed of movement of the ridge does not allow time for the surface high-pressure system to develop as strongly and as frequently to sustain the Santa Ana winds. Also, the presence of stronger uplift near the coast of southern California in the omega analysis of El Niño is most likely a signature of an increase in winter cyclones in the southwestern United States compared to non-El Niño winters. The southeastern quadrant of the stronger and more expansive Aleutian Low during El Niño often produces more cyclones that pass through southern California during winter (Raphael and Mills 1996), which can hinder the Santa Ana wind development.

Although the major findings in March correspond to the decrease in frequency of the late-

winter wind events in Raphael's (2003) study, signals of strong El Niño winters typically influence the entire winter season, which is defined by Su, Neelin, and Chou (2001) and Monteverdi and Null (1997) as January through March. Perhaps the differences in extratropical responses to El Niño among specific events play a role in the results, and this variability among El Niño events, as noted in Schonher and Nicholson's (1989) and Fu, Diaz, and Fletcher's (1986) research, may create inconsistent results for some winter months during the seven El Niño winters used in this study. Schonher and Nicholson classified El Niño events as wet, normal, and dry because El Niño produced varying amounts of precipitation from one event to another. Therefore, El Niño events may elicit different responses from the atmospheric circulation, and these different responses may make an average of only seven El Niño events not the optimal data set. Despite the limitations of the data, the results do show that the effect of El Niño is to decrease the duration and frequency of events in March. The large-scale circulation patterns that contribute to this reduction seem clear, but a larger sample size may provide statistically significant results for the entire winter season. In addition, as the data set lengthens in the future, research should consider Schonher and Nicholson's (1989) classifications of various El Niño types and the corresponding responses of the Santa Ana winds. ■

Literature Cited

- Daily Weather Maps*, 1968–2000, NCDC Cooperative Station Data. National Climate Data Center, CD-ROM.
- Fedorov, A. V., and S. G. Philander. 2000. Is El Niño changing? *Science* 288:1997–2001.
- Fosberg, M. A., C. A. O'Dell, and M. J. Schroeder. 1966. *Some characteristics of the three-dimensional structure of Santa Ana winds*. U.S. Forest Service Research Paper PSW-30, Pacific Southwest Forest and Range Experiment Station, Berkeley, CA, 26 pp.
- Fu, C., H. F. Diaz, and J. O. Fletcher. 1986. Characteristics of the response of SST in the central Pacific associated with warm episodes of the Southern Oscillation. *Monthly Weather Review* 114:1716–38.
- Goudie, A. S. 2001. *Environmental change and human society*. New York: Oxford University Press.
- Kalnay, E., M. Kanamitsu, R. Kistler, W. Collins, D. Deaven, L. Gandin, M. Iredell, et al. 1996. The

- NCEP/NCAR 40-yr reanalysis project. *Bulletin of the American Meteorological Society* 77:437–71.
- Klemp, J. B., and D. K. Lilly. 1975. The dynamics of wave-induced downslope winds. *Journal of Atmospheric Science* 32:320–38.
- Legler, D. M. 1998. *ENSO Index according to JMA SSTA (1868–present)*. Center for Ocean-Atmospheric Prediction Studies. http://www.coaps.fsu.edu/products/jma_index.php (last accessed 7 December 2006).
- Livezey, R. E., M. Masutani, A. Leetmaa, H. L. Rui, M. Ji, and A. Kumar. 1997. Teleconnective response of the Pacific/North American region atmosphere to large central equatorial Pacific SST anomalies. *Journal of Climate* 10:1787–1820.
- Minnich, R. A. 1983. Fire mosaics in southern California and northern Baja California. *Science* 219: 1287–94.
- Monteverdi, J., and J. Null. 1997. El Niño and California precipitation. Western Region Technical Attachment no. 97-37, 21 November.
- Raphael, M. N. 2003. The Santa Ana Winds of California. *Earth Interactions* 7:1–13.
- Raphael, M. N., and G. M. Mills. 1996. The role of mid-latitude cyclones in the winter precipitation of California. *Physical Geography* 48:251–62.
- Ropelewski, C. F., and M. S. Halpert. 1987. Global and regional scale precipitation patterns associated with the El Niño–Southern Oscillation. *Monthly Weather Review* 115:1606–26.
- Scheetz, V. R., J. R. Henz, and R. A. Maddox. 1976. *Colorado severe downslope wind-storms, a prediction technique*. Final report to Techniques Development Laboratory, National Weather Service, NOAA, DOC, Contract 5-35421.
- Schonher, T., and S. E. Nicholson. 1989. The relationship between California rainfall and El Niño events. *Journal of Climate* 2:1258–69.
- Sommers, W. T. 1978. LFM forecast variables related to Santa Ana wind occurrences. *Monthly Weather Review* 106:1307–16.
- Su, H., J. D. Neelin, and C. Chou. 2001. Tropical teleconnection and local response to SST anomalies during the 1997–1998 El Niño. *Journal of Geophysical Research* 106 (D17): 20,025–20,043.
- JASON FINLEY completed his M.A. in Geography in the Department of Geography at the University of California, Los Angeles, Los Angeles, CA 90095. E-mail: j_p_finley@hotmail.com. His research interests include climatology of California and geographic information systems.
- MARILYN RAPHAEL is a Professor of Geography in the Department of Geography at the University of California, Los Angeles, Los Angeles, CA 90095. E-mail: raphael@geog.ucla.edu. Her research interests include climate dynamics, California climate and Antarctic sea ice-atmosphere interactions.